

Journal Pre-proof

In vitro and in vivo efficacy evaluation of new self-assembling curcumin loaded nanohyaluronan-glycosomes on wound restoring in health and diabetic rats

Francisco José Gómez García, Antonio Ramírez Andreo, Maria Manconi, María Letizia Manca, Pietro Matricardi, Chiara di Meo, Xavier Fernández-Busquets, Francisco Martínez Díaz, Diego Salmerón, Pía López Jornet



PII: S0141-8130(25)05251-1

DOI: <https://doi.org/10.1016/j.ijbiomac.2025.144699>

Reference: BIOMAC 144699

To appear in: *International Journal of Biological Macromolecules*

Received date: 1 January 2025

Revised date: 19 April 2025

Accepted date: 25 May 2025

Please cite this article as: F.J.G. García, A.R. Andreo, M. Manconi, et al., In vitro and in vivo efficacy evaluation of new self-assembling curcumin loaded nanohyaluronan-glycosomes on wound restoring in health and diabetic rats, *International Journal of Biological Macromolecules* (2024), <https://doi.org/10.1016/j.ijbiomac.2025.144699>

This is a PDF file of an article that has undergone enhancements after acceptance, such as the addition of a cover page and metadata, and formatting for readability, but it is not yet the definitive version of record. This version will undergo additional copyediting, typesetting and review before it is published in its final form, but we are providing this version to give early visibility of the article. Please note that, during the production process, errors may be discovered which could affect the content, and all legal disclaimers that apply to the journal pertain.

***In vitro* and *in vivo* efficacy evaluation of new self-assembling curcumin loaded nanohyaluronan-glycosomes on wound restoring in health and diabetic rats**

Francisco José Gómez García^{1*}, Antonio Ramírez Andreo², Maria Manconi³, María Letizia Manca^{3*}, Pietro Matricardi⁴, Chiara di Meo⁴, Xavier Fernández-Busquets⁵, Francisco Martínez Díaz⁶, Diego Salmerón⁷, Pía López Jornet⁸.

- a. DSD. Stomatology. Faculty of Medicine. University of Murcia, Murcia, Spain.
- b. MD. Dermatology. University Hospital Reina Sofía, Murcia, Spain.
- c. Department of Scienze della Vita e dell'Ambiente, Drug Science Division, University of Cagliari, Cagliari, Italy.
- d. Department of Drug Chemistry and Technologies, Sapienza University of Rome, Rome 00185, Italy.
- e. Institute for Bioengineering of Catalonia, The Barcelona Institute of Science and Technology, Barcelona, Spain.
- f. MD. Pathology. University Hospital Reina Sofía, Murcia, Spain.
- g. Departamento de Ciencias Sociosanitarias, Universidad de Murcia, Murcia, Spain.
- h. MD. Stomatology. Faculty of Medicine. University of Murcia, Murcia, Spain.

The authors declare no funding neither conflict of interest

*Corresponding author:

Maria Letizia Manca. Dept. Of Life and Environmental Sciences, University of Cagliari, Italy. Office Phone +390706758582, email: mlmanca@unica.it

Francisco José Gómez García. Clínica Odontológica Universitaria. HU Morales Meseguer. Avda Marqués de los Vélez s/n. 30008, Murcia, Spain. Tlf: +34868889443, e-mail: fjgomez@um.es.

Abstract

In this study the wound healing efficacy of new self-assembling curcumin loaded nanohyaluronan-glycosomes has been tested in healthy and diabetic rats. Curcumin was loaded in nanohyaluronan-liposomes and -glycosomes, special vesicles obtained mixing curcumin, hyaluronan nanohydrogel and soy lecithin. Curcumin loaded liposomes and glycosomes were also prepared, characterized and tested as references. The physico-chemical (size and size distribution, surface charge and morphology), and technological (entrapment efficiency, stability over time and skin delivery) characteristics and biological performances (safety, ability to protect *in vitro* cells from oxidative damage) of prepared formulations were

measured. Finally, they were daily applied to skin wounds of healthy or diabetic rats. The animal skin was excised and analysed at days 3, 7 and 14. The macroscopic observation underlined the higher ability of curcumin loaded nanohyaluronan-glycosomes to improve wound healing in diabetic rats, already on day 3 up to day 14 ($p < 0.05$). Histopathological analysis confirmed an accelerated re-epithelization in healthy rats, while increased angiogenesis in diabetic ones. The superior therapeutic efficacy of curcumin loaded nanohyaluronan-glycosomes compared to other formulations can be related to their enhanced ability to deliver higher curcumin concentrations at the wound site due to a synergistic effect of glycerol, hyaluronan nanohydrogel and lecithin.

Key words: wound healing; rats; curcumin; liposomes; hyaluronic acid; diabetic wounds; nanohydrogel.

1. Introduction

The skin is a dynamic structure whose main function is to act as a physical barrier, controlling the regulation of permeability, body temperature and protecting against infectious microorganisms, toxic chemicals, ultraviolet radiations and physical insults [1]. It is also implicated in wound repair and regeneration processes, which are impaired in different local or systemic disease conditions such as inflammatory skin disorders, cardiovascular problems, obesity, and diabetes [2]. The last is one of the main causes of skin wounds in the world and, being this pathology steeply rising, instances of chronic or hard-healing ulcers are expected to increase. The two most common types of diabetes are type 1 and type 2 and the former constitute more than 90% of cases. It is usually known as diabetes mellitus and is a metabolism disorder affecting carbohydrates, proteins and lipids and causing hyperglycemia, which chronically damages blood vessels and impairs proper blood perfusion. These peripheral vascular problems associated with neuropathy, facilitated wound formation, often triggered by minor traumas, and made recovery more challenging [3]. Indeed, chronic hyperglycemia of diabetic patients contributes to the formation of advanced glycation end products, which reduce skin collagen solubility causing macro- and micro-angiopathy, decreasing phagocytosis and in turn the bactericidal capacity of leukocytes leading a slowed down healing process [2]. Currently, there is no effective and suitable therapy for the successful treatment of diabetic wounds, which contributes to morbidity, impairs quality of life, and may lead to amputation of lower extremities. These wounds also have significant negative consequences for patients and healthcare systems, resulting in high medical costs. [4].

Actually, wound healing represents a significant therapeutic medical, social, and economic challenge for clinicians and researchers worldwide due to the complexity of the involved processes that often fails to progress. Natural products offer new prospects in the development of alternative therapeutic treatments for chronic skin lesions. Especially, polyphenols fully respond to this need thanks to their great biological potential as antioxidants, anti-inflammatories, and antimicrobics [5–7]. One of the most studied and promising polyphenols is curcumin, extracted from *Curcuma longa* (turmeric), that has been widely used not only in Indian and Chinese cuisine but also in traditional medicine as an herbal remedy in a range of disorders [8]. This molecule [1,7-bis (4-hydroxy-3-methoxyphenyl)-1,6-heptadiene-3,5-dione] is lipophilic, has

antioxidant, anti-aging, anti-inflammatory, anti-mutagenic, and anti-infective properties, and is usually and successfully used in the treatment of skin wounds [8–10]. Previous studies have demonstrated its ability to accelerate the healing process by reducing oxidative developments, especially lipid peroxidation, through the neutralization of free radicals or reactive oxygen species (ROS). This beneficial effect is reinforced by the ability to increase the activity of catalase, glutathione peroxidase and superoxide dismutase [9,11]. Synergically, thanks to its anti-inflammatory properties, curcumin suppresses the production and activation of various cytokines such as α -tumour necrosis factor (TNF- α), interleukin 1 (IL-1) and KB-necrosis factor (NF-kB) [12]. Unfortunately, curcumin does not easily pass through the biological membranes and is rapidly metabolized and eliminated, resulting in poor bioavailability and low serum and tissue levels, that limit its clinical applications [13]. To improve local and skin delivery, a huge number of formulations have been developed and tested including hydrogels, films, patches, fibres, and several nano-carriers [14]. Among the different nano-carriers, phospholipid vesicles, specifically engineered for skin applications, have demonstrated advanced performances, providing solutions that meet the demands of payload delivery and formulation safety [15]. In a previous study, curcumin was loaded in sodium hyaluronate immobilized vesicles, so called hyalurosomes, that fully restored the structural and functional conditions of damaged skin [16,17].

Considering these challenges and outcomes, in the present study curcumin was loaded in hyaluronan-cholesterol nanohydrogel supramolecularly assembled with liposomes or glycerosomes (nanohyaluronan-liposomes or nanohyaluronan-glycerosomes). The main physico-chemical and technological characteristics of vesicles (morphology, size, zeta potential, encapsulation efficiency, stability) were measured. Vesicle ability to facilitate payload accumulation in the intact skin was tested *in vitro* as a function of time. *In vitro* biocompatibility of formulations and their ability to protect cells from damages induced by oxidative stress were evaluated. Their effectiveness in speeding up skin reepithelization and wound healing was assessed *in vitro* on human keratinocytes and fibroblasts and *in vivo* using diabetic and non-diabetic rats.

2. Materials and Methods

2.1. Materials

A commercial mixture of soy phosphatidylcholine (94–102%) and monoacyl phosphatidylcholine (less than 4%) called Phospholipon[®]90G was purchased from

Lipoid GmbH (Ludwigshafen, Germany). Hyaluronan tetrabutylammonium salt (HA-TBA⁺, molecular weight = 2.2×10^5) was purchased from Hysilk (Dolní Dobrouč, Czech Republic). Curcumin, cholesterol, MTT (3-[4,5-dimethylthiazol-2-yl]-2,5-diphenyl tetrazolium bromide), streptozotocin and all the other reagents of analytical grade were purchased from Sigma-Aldrich-Merck (Milan, Italy). Cell medium, foetal bovine serum, penicillin, and streptomycin, fungizone, and all the other reagents used for cell studies were purchased from Thermo-Fisher Scientific Inc (Waltham, Massachusetts, USA).

2.2. Hyaluronan-cholesterol synthesis and preparation of nanohydrogel

The synthesis of hyaluronan-cholesterol derivative was carried out according to a previously developed procedure [18]. Hyaluronan tetrabutylammonium salt (500 mg) was added to 10 mL of *N*-methyl-2-pyrrolidone and left under stirring at 25 °C for 5 h; then, cholesterol (65 or 39 mg), solubilised in 2 mL of *N*-methyl-2-pyrrolidone, was added and the reaction was left under stirring for 48 h at 38 °C. 2 mL of sodium chloride (saturated solution) were added drop by drop to the mixtures, which were left under stirring for 30 min to replace tetrabutylammonium ions with sodium ones. A mixture of acetone and water (90:10, v/v) was added (4 times the reaction volume) and left for 1 h at 4 °C. The precipitated cholesterol-hyaluronan was separated, dispersed in bi-distilled water, and finally dialysed against water (cellulose membrane tubing, molecular weight cut-off: $1.2\text{--}1.4 \times 10^4$ Da, Sigma-Aldrich, Darmstadt, Germany) until constant conductivity was reached. Samples were freeze-dried with a “Modulyo 4K” Edwards High Vacuum equipment, yielding 350 mg of white solid (70% mass recovery). To prepare the nanohydrogel, hyaluronan-cholesterol (20 mg) was dispersed in 10 mL of phosphate buffer (PBS) at pH 7.0 or in a mixture (1:1) of glycerol and PBS and autoclaved at 120 °C for 1 h.

2.3. Preparation and characterization of vesicles

In a typical formulation of nanohyaluronan-liposomes and nanohyaluronan-glycerosomes, curcumin (20 mg) was dispersed in 2 mL of hyaluronan-cholesterol nanohydrogel, previously prepared in PBS or in a mixture of glycerol and PBS (1:1) (see nanohydrogel preparation). The dispersions were sonicated for 99 cycles of 5 s, alternating with 2-s pauses, using the Soniprep 150 ultrasonic disintegrator (MSE Crowley, United Kingdom). Finally, the phospholipid P90G (440 mg) was added, and

the dispersion was sonicated again performing 25 cycles of 5 s, alternating with 5 s of pause, using the same Soniprep 150 ultrasonic.

Alternatively, curcumin (20 mg) and P90G (440 mg) were dispersed in 2 mL of PBS to prepare liposomes or in 2 ml of a mixture of glycerol and PBS (1:1) to prepare glycerosomes. The dispersions were sonicated performing 25 cycles of 5 s, alternating with 5 s of pause, using a Soniprep 150 ultrasonic disintegrator.

This preparation has been chosen as it allows the components to be dispersed directly in the dispersing medium, avoiding the use of organic solvents, resulting in formulations that are easily reproducible on a large scale and more reliable in terms of safety and quality, without the need of further steps.

Labelled nanohyaluronan-liposomes and nanohyaluronan-glycerosomes were obtained mixing (5(6)-carboxyfluorescein (0.025 mg/ml) together with curcumin and hyaluronan-cholesterol nanohydrogels, sonicating the dispersions, then adding the fluorescent phospholipid (1,2-dioleoyl-sn-glycero-3-phosphoethanolamine-N-lissamine-sulfo-rhodamineB; 0.035 mg/ml) and sonicating again, as above. Regarding labelled liposomes and glycerosomes, (5(6)-carboxyfluorescein (0.025 mg/ml) has been added together with curcumin and the fluorescent phospholipid (1,2-dioleoyl-sn-glycero-3-phosphoethanolamine-N-lissamine-sulfo-rhodamineB; 0.035 mg/ml) and processed as reported above.

The average diameter, polydispersity index, and zeta potential of the vesicles were measured using a ZetasizerUltra (Malvern, Worcestershire, United Kingdom), as previously reported [19].

The curcumin non incorporated inside the vesicles was separated by dialysis, transferring the dispersions (1 mL) in Spectra-Por membranes with 12–14 kDa MW cut-off, 3 nm pore size (Spectrum Laboratories Inc., DG Breda, The Netherlands) and dialyzing in 2 L of water for 2 h, refreshing the water at 1 h. The content of curcumin in vesicle dispersions before and after the dialysis was quantified by ultra-performance liquid chromatography (UPLC).

Stability studies have been performed as well, by monitoring the main physico-chemical properties (size, size distribution and surface charge) of samples stored for 12 months at 4 °C in dark glass vials to protect them from light and improve their shelf life.

2.4. Analytical method

Curcumin was quantified by means of ultra-performance liquid chromatography (UPLC, ACQUITY H-class Plus system, Waters Corporation, Milan, Italy) using a chromatograph equipped with a UV photodiode array detector and a C18 reverse phase column (Waters Corporation, 1.7 μm , 2.1 mm \times 50 mm), at 25 °C. A mobile phase of water, methanol and acetic acid (49:50:1) was used. 25 μL of samples were injected, the flow rate was set at 1 mL/min and curcumin was detected at 425 nm. Stock solutions of curcumin at different concentrations were prepared using the mobile phase as solvent. The calibration curve obtained plotting peak areas of standard solutions of curcumin versus concentrations (from 0.05 to 20 $\mu\text{g/mL}$) had a correlation coefficient (R_2) of 0.9998.

2.5. *In vitro* skin delivery studies with fluorescent labelled vesicles

The vesicles were labelled with a fluorescent phospholipid (1,2-dioleoyl-sn-glycero-3-phosphoethanolamine-N-lissamine-sulfo-rhodamineB; 0.035 mg/ml) and loaded with a hydrophilic fluorescent marker (5(6)-carboxyfluorescein; 0.025 mg/ml), as reported above (paragraph 2.3.) [20]. Fluorescent vesicles (100 μL) were applied on the dorsal skin of new-born pigs sandwiched between the donor and receptor compartment of Franz diffusion cells [20]. At regular time intervals (2, 4, and 8 h) the solution of receptor compartment was changed to ensure the sink conditions. At 8 h skin specimens were removed, and the diffusion area was cut and frozen at -80 °C. Sections of the skin (7 μm thickness) were cut with a cryostat (Leica CM1950, Barcelona, Spain) and observed using a FluoView FV1000 inverted confocal microscope (Olympus, Barcelona, Spain) equipped with a light laser and an UplanSApo 20 \times objective NA 0.75. (5(6)-carboxyfluorescein was excited at 600 nm and detected at 640 nm; fluorescent phospholipid was excited at 559 nm and detected at 578 nm.

2.6. *In vitro* cytocompatibility and protective effect against oxidative damages

Human keratinocytes (HaCaT) and 3T3 mouse fibroblasts (ATCC collection, Manassas, VA, US) were grown as monolayers under 100% humidity and 5% carbon dioxide at 37 °C in Dulbecco Modified Eagle medium containing 10% foetal bovine serum, 1% penicillin, streptomycin and fungizone. To measure the viability, cells (7.5×10^3 cells/well) were seeded in 96-well plates and incubated in the previous culture conditions for 24 h. Thereafter, medium was withdrawn, and curcumin samples, diluted with fresh medium up to 10, 1, 0.1 $\mu\text{g/mL}$, were added and left for 48 h. Then MTT

solution (0.5 mg/mL final concentration) was added to each well and replaced with dimethyl sulfoxide after 3 h of incubation. The absorbance was measured at 570 nm with a microplate reader (Multiskan EX, Thermo Fisher Scientific Inc., Waltham, MA, US) and cell viability was calculated as a percentage of live cells versus untreated control cells (100% viability).

To assess the efficacy of the formulations in preventing hydrogen peroxide-induced cell death, cells were maintained in 96-well plates for 24 hours, then stressed with hydrogen peroxide (1:50000 dilution of water solution 30%; Sigma-Aldrich/Merck, Milan, Italy) and treated with samples adjusted to a final concentration of 0.1 µg/mL of curcumin in the medium. At 4 h, the MTT was added, replaced with dimethyl sulfoxide after 3 h of incubation and absorbance was measured at 570 nm, then cell viability was calculated as above. Untreated cells (100% viability) were used as a positive control, and those stressed with hydrogen peroxide and unprotected with curcumin samples were used as a negative control.

2.7. *In vitro* scratch assay

The ability of curcumin samples to stimulate cell proliferation and migration was assayed observing and measuring the closure of a linear scratch generated in cell monolayer (scratch assay). Cells were cultured in 6-well plates and when the complete confluence was reached, a linear scratch was produced with a sterile plastic pipette tip. The scattered cells were removed by gently washing with fresh medium and medium containing the samples diluted up to 0.1 µg/ml of curcumin were added. Cells were incubated for 48 h. Untreated cells were used as controls. The lesions were observed with an optical microscope (10 × objective) and the images were captured immediately after the addition of samples and at 24, and 48 h.

2.8. *In vivo* assay

Sixty-three male Sprague-Dawley rats weighing 140-184 g from the experimental animal housing facilities of the University of Murcia (Murcia, Spain) were used in the study. The animals were housed in cages with a 12:12 h light-darkness cycle, a mean temperature of 22 °C, and a relative humidity of 40-70%. Food and water were made available *ad libitum*. The rats were handled in accordance with applicable legislation regarding the protection of animals used in experimental studies (Directive 2010/63/EU and Spanish Royal Decree 53/2013 of 1 February 2013). The study was approved by the

Bioethics Committee of the University of Murcia (Ref. code A13170104), and the investigation was carried out in accordance with the ARRIVE guidelines (Animal Research: Reporting of *In Vivo* Experiments).

2.9. Induction of diabetes

The rats received an intraperitoneal dose of 30 mg/kg of streptozotocin, administered as three pulses spaced 48 hours apart. Capillary blood glucose was determined on the day following each administered dose. Animals presenting blood glucose levels > 200 mg/dl were considered to be diabetic. The skin wounds were made 4 weeks after the induction of diabetes, and the blood glucose levels were monitored throughout the study. In order to calculate a representative sample size, a power of 80% was required (5% alpha level). A total of 63 rats were used (45 healthy animals and 18 diabetic animals), randomized using a software application to the following groups of 9 animals each: Group 1, healthy animals treated with curcumin loaded liposomes; Group 2, healthy animals treated with curcumin loaded glycosomes; Group 3, healthy animals treated with curcumin loaded nanohyaluronan-liposomes; Group 4, healthy animals treated with curcumin loaded nanohyaluronan-glycosomes; Group 5, healthy animals untreated (control group); Group 6, diabetic animals untreated (control group); Group 7, diabetic animals treated with curcumin loaded nanohyaluronan-glycosomes.

2.10. Skin wounds, treatments and sample collection

Four wounds were made in the shaven dorsal skin of each animal using an 8-mm punch, under inhalatory general anaesthesia (isoflurane) and local anaesthesia with 2% lidocaine by subcutaneous injection. The epidermis and dermis and part of the subcutaneous cellular tissue were removed without reaching the fascial layer. The skin fragments were removed with a scalpel. The topical treatments were applied daily with a Pasteur pipette, covering the entire wound surface. At day 3, 7 and 14 by surgery, the material for the macroscopic (digital photographs) and microscopic studies (tissue samples) was separated. The general physical condition of the animals and their body weight were also monitored at these timepoints. Post surgery, at day 3, 7 and 14, three animals of each group were sacrificed in a carbon dioxide chamber, digital photographs of the wounds were taken, and skin samples were collected, fixed in formalin solution and embedded in paraffin for histopathological study of the wounds. The animals not sacrificed were sedated for photographic recording on those same days.

2.11. Macroscopic study

After producing the wounds (day 0) and on day 3, 7 and 14, digital photographs of the rats were obtained alongside millimetered paper, with the camera at a distance of 20 cm from the skin, using a fixed tripod mounting. The images obtained were analysed using ImageJ software, following morphological calibration, to determine the lesion area and compare it among the different groups and at the different timepoints.

2.12. Microscopic study

The tissue samples were fixed in buffered 4% formalin solution for at least 48 h and embedded in paraffin, followed by the obtainment of 3 μm sections that were stained with hematoxylin-eosin and Masson trichrome stain in the Department of Pathology of Hospital Universitario Reina Sofía (Murcia, Spain). A semiquantitative histopathological study of the samples was made, based on the classification of Abramov (scoring the following parameters from 0-3: angiogenesis, granulation tissue, collagen accumulation and inflammation) [21]. Angiogenesis was assessed according to the number of vessels per high magnification field (0 = none; 1 = up to 5; 2 = between 6-10; and 3 = over 10).

The maturation of granulation tissue in turn was scored based on the distribution of fibroblasts. These cells were considered to be mature when they presented a small and elongated nucleus and were distributed forming parallel bands, while immature fibroblasts were defined by a “stellate” or epithelioid morphology. In relation to the accumulation of collagen, both the amount, thickness and distribution of the collagen fibres was considered. Inflammation was defined as the presence of neutrophils and eosinophils, plasma cells and histiocytes in the wound.

Re-epithelization and neovascularization were measured manually from margin to margin of the wound using the ImageJ program, recording the distance between margins (in μm) as a quantitative variable in all the samples. In the case of neovascularization, a histomorphometry study of the vessels was carried out, tracing the contour of the vessels present in three randomly selected wound areas of 100 μm^2 . The ImageJ analysis allowed the quantification of the area occupied by blood vessels in the tissue repair zone. First, images of the study zones under 20x magnification were obtained, followed by morphological calibration and manual tracing of the contour of each of the identified vessels. The program automatically calculated the perimeter and total area in each image, and the numerical data were transferred to Microsoft Excel spreadsheets.

This parameter was only evaluated in the samples from diabetic rats and the healthy controls (groups 5, 6 and 7).

2.13. Immunohistochemical study

Immunohistochemical study was only made in the diabetic rats and was carried out at the Department of Pathology of Hospital Universitario Reina Sofía (Murcia, Spain). First, the samples were deparaffinized with the OMNIS-DAKO system (Agilent), and pre-treatment was carried out with EnVision FLEX, Low pH (Ref. GV805) (heat-induced epitope retrieval [HIER]) during 30 min. The ready to use antibody was incubated for 20 min with a FLEX Negative Control, Rabbit (Ref. GA600) at the same time. Visualization was carried out with EnVision FLEX (Ref. GV800) + EnVision FLEX + Rabbit LINKER (Ref. GV809) in a block during 3 min of Link: 10 min; polymer: 20 min; and chromogen: 5 min. Counterstaining with hematoxylin was then made (Ref. GC808), with an incubation time of three minutes. After staining, dehydration, rinsing and mounting of the slides were performed with permanent mounting medium (Eukitt®). All the deparaffinization, rehydration and antigen retrieval, antibody incubation, rinsing and visualization steps were performed with the Dako Omnis system. The primary antibodies used were monoclonal antibodies targeted to PCNA, CD34, TIMP-1 and MMP9 (Dako, S.A., Barcelona, Spain) at 1:200 dilution during 40 min.

In the case of PCNA, quantitative assessment of the nuclei was made, that proved positive for this antibody at the wound margins. The ImageJ program was used to select the epidermal margin of the wound, and the total area of the field, the area occupied by nuclei, and the area occupied by positive nuclei were recorded. This technique was applied to both healthy and diabetic rats (i.e., the healthy controls and diabetic controls – not in the rats that received treatment). Semiquantitative assessment was made in the case of the rest of the antibodies, based on a scale from 0-3 (0 = no staining, 1 = mild staining, 2 = moderate staining, 3 = intense staining).

2.14. Statistical analysis

A descriptive study was made of each variable. Analysis of variance (ANOVA) and the Kolmogorov-Smirnov test were used with the quantitative variables to determine whether the variations were homogeneous in each case. Statistical significance was

considered for $p \leq 0.05$. The SPSS version 20.0 statistical package (SPSS® Inc., Chicago, IL, USA) was used throughout.

3. Results

3.1. Preparation and characterization of vesicles

Nanohyaluronan-liposomes and nanohyaluronan-glycosomes were prepared combining curcumin, phosphatidylcholine and hyaluronan-cholesterol nanohydrogel prepared in PPS or in PBS and glycerol. The corresponding liposomes or glycosomes without nanohydrogel were prepared as comparison to understand the possible effect caused by the nanohydrogel addition. Their mean diameter, polydispersity index, zeta potential and entrapment efficiency were measured (Table 1). Liposomes were sized 185 ± 20 nm and slightly polydisperse, glycosomes were significantly larger, 500 ± 34 nm, and more polydispersed. The addition of hyaluronan-cholesterol nanohydrogel in the water medium caused an enlargement of mean diameter of liposomes (305 ± 37 nm) while that of glycosomes remained unchanged (543 ± 39 , $p > 0.05$ versus the value of glycosomes). Notwithstanding the high value of polydispersity index, it was always repeatable, as confirmed by the low standard deviation obtained from at least 6 repetitions. Stability studies, conducted by monitoring key physico-chemical parameters (mean diameter, polydispersity index, and surface charge) over 12 months of storage at 4°C , confirmed the high stability of the tested formulations, with no significant changes observed (variations $< 15\%$), particularly for nanohyaluronan-liposomes and nanohyaluronan-glycosomes. The only exception was conventional liposomes, which exhibited a marked increase in both mean diameter and polydispersity index ($> 40\%$ increase) (data not shown).

Table 1. Mean diameter (MD), polydispersity index (PI), zeta potential (ZP) and entrapment efficiency (EE) of curcumin loaded liposomes, glycosomes, nanohyaluronan-liposomes and nanohyaluronan-glycosomes. Each value represents the average \pm standard deviation of at least six determinations ($n=6$).

Sample	MD (nm)	PI	ZP (mV)	EE (%)
Liposomes	185 ± 20	0.32 ± 0.02	-33 ± 3	73 ± 9
Glycosomes	500 ± 34	0.38 ± 0.04	-40 ± 6	71 ± 8
Hyaluronan-liposomes	305 ± 37	0.37 ± 0.03	-44 ± 9	81 ± 6

Hyaluronan-glycosomes	543±39	0.39±0.04	-59±5	80±9
-----------------------	--------	-----------	-------	------

The actual formation of the self-assembling curcumin loaded nanohyaluronan-vesicles, and their aggregation structure were observed with a cryo-transmission electron microscope (Figure 1), which provides reliable images without alterations [22]. According to the high polydispersity index, the size of vesicles was not homogenous and the smaller were almost unilamellar while the larger were multilamellar and multicompartiment, as previously found by loading curcumin at high concentrations [23]. The addition of the hyaluronan-cholesterol nanohydrogel in the hydrating medium of vesicles did not significantly affect their morphology and structure, as previously found by Manconi et al. [24].

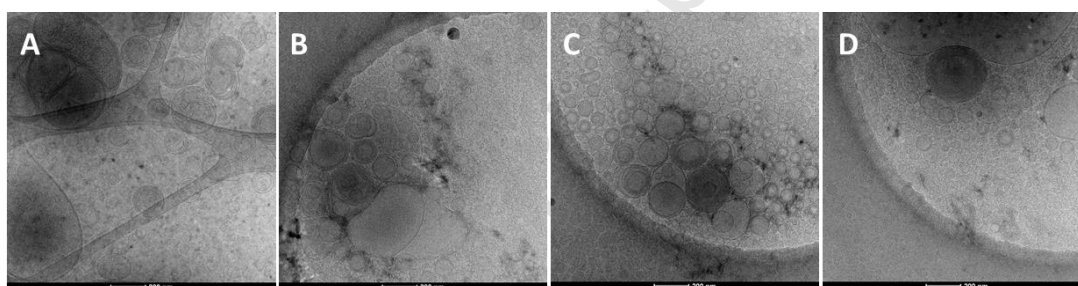


Figure 1. Representative Cryo-TEM images of curcumin loaded liposomes (A), glycosomes (B), nanohyaluronan-liposomes (C) and nanohyaluronan-glycosomes (D).

The ability of formulation to cross the skin was evaluated using vesicles labelled with a fluorescent phospholipid and a hydrophilic marker (Figure 2). When liposomes were used a few green fluorescence of hydrophilic probe was observed in the stratum corneum and in the dermis. Using glycosomes the green fluorescence was distributed in the whole epidermis and dermis. Treating the skin with nanohyaluronan-liposomes a few red fluorescence of phospholipid was visible on the skin surface, while in the dermis a yellow coloration due to the superposition of red and green was detected, denoting the simultaneous presence of the two main components of vesicles. A similar behaviour was observed using nanohyaluronan-glycosomes, but in this case the yellow colour in the dermis was more intense.

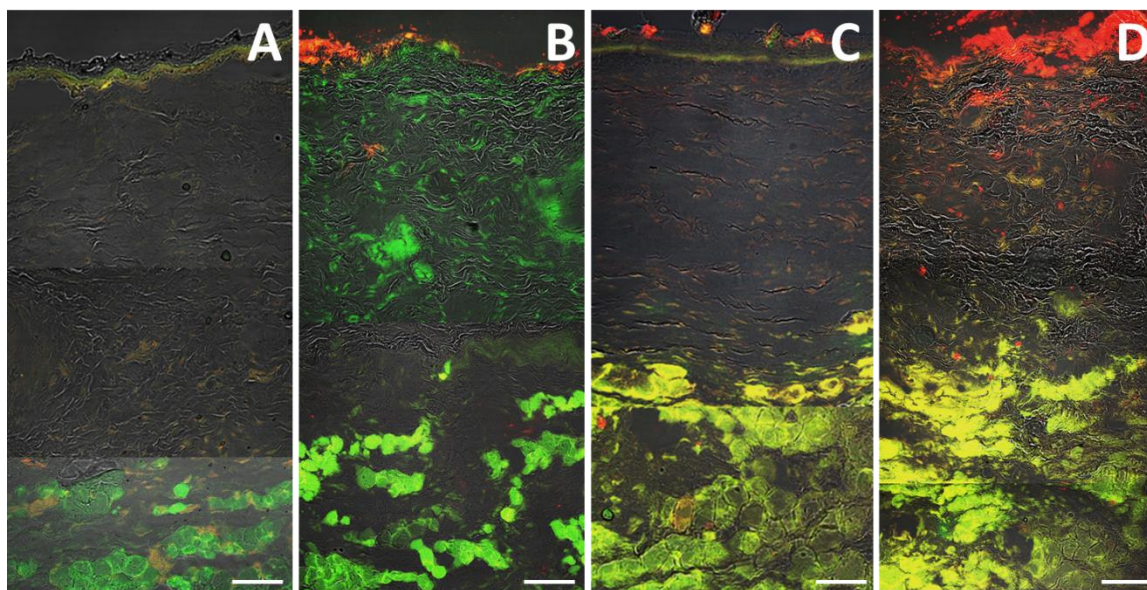


Figure 2. Representative confocal images of skin sections treated for 8 h with curcumin loaded liposomes (A), glycosomes (B), nanohyaluronan-liposomes (C) and nanohyaluronan-glycosomes (D) fluorescently labelled with lipophilic 1,2-dioleoyl-sn-glycero-3-phosphoethanolamine-N-lissamine-sulfo-rhodamineB (red colour) and hydrophilic 5(6)-carboxyfluorescein (green colour). Scale bars: 100 μm .

***In vitro* studies with cells**

Keratinocytes and fibroblasts were used as they are the main representative cells of the skin. The biocompatibility of formulations was assayed adding the formulations in the cell medium at different dilutions (Figure 3).

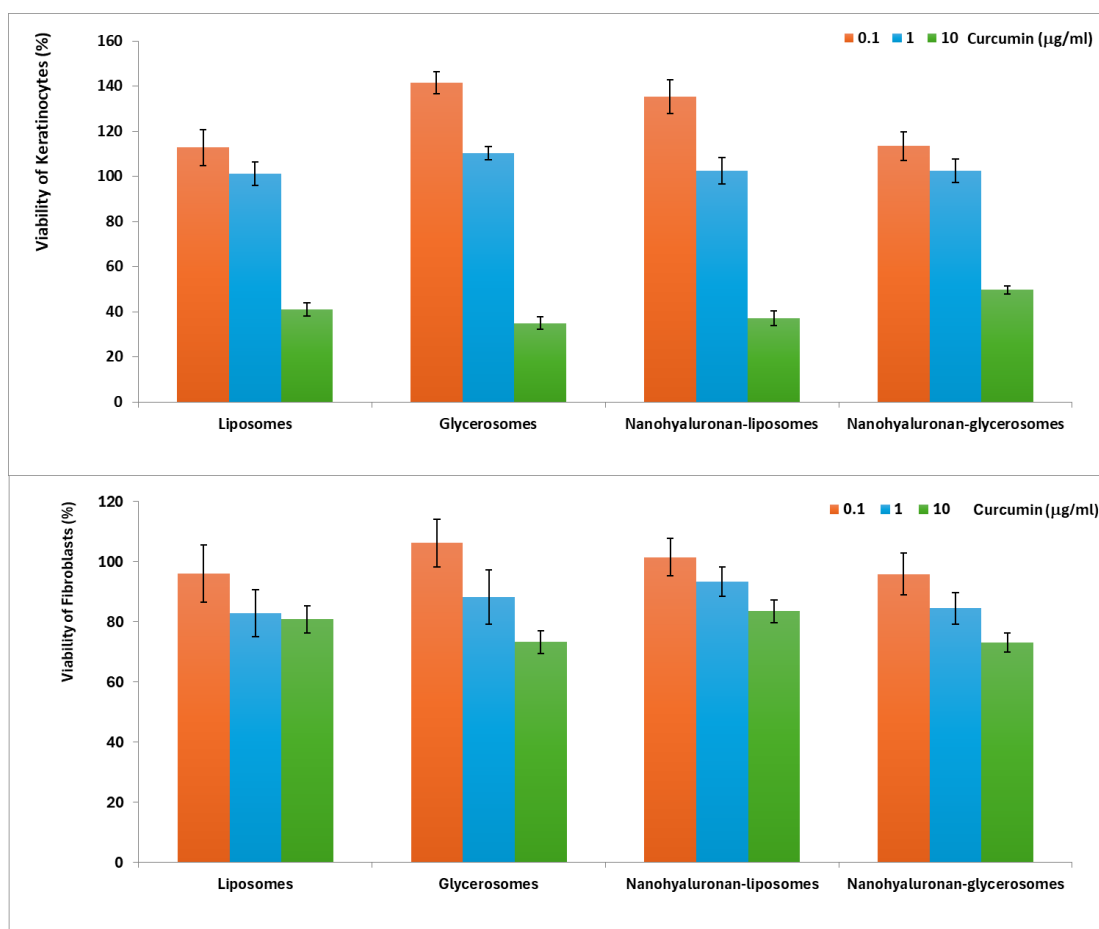


Figure 3. Viability of keratinocytes and fibroblasts incubated for 48 h with curcumin loaded liposomes, glycosomes, nanohyaluronan-liposomes and nanohyaluronan-glycosomes. Each value represents the mean value \pm standard deviation of at least six determinations ($n=6$).

The viability of keratinocytes treated with the highest concentration of curcumin (10 $\mu\text{g/ml}$) significantly decreased up to 40% denoting a toxicity. Using the other concentrations of curcumin (0.1 and 1 $\mu\text{g/ml}$) the viability of these cells was always $\geq 100\%$, confirming their biocompatibility. Results indicated no toxicity of formulations against fibroblasts, the viability was $\approx 100\%$ using the lowest concentration of curcumin and $\approx 80\%$ using the higher concentrations of it (1 and 10 $\mu\text{g/ml}$). Since a cell mortality of $\leq 20\%$ is generally accepted as indicative of biocompatibility, the tested formulations can be considered biocompatible [25]. The results suggest that the biocompatibility of curcumin samples was strictly dependent on used concentration and cell type. Specifically, keratinocytes were more affected by the curcumin formulations, especially

at the highest concentration (10 mg/mL) as their viability was strongly reduced. This concentration was considered toxic, and the further *in vitro* efficacy test was performed using the less concentrated samples (0.1 mg/mL of curcumin), that were highly biocompatible with both keratinocytes and fibroblasts.

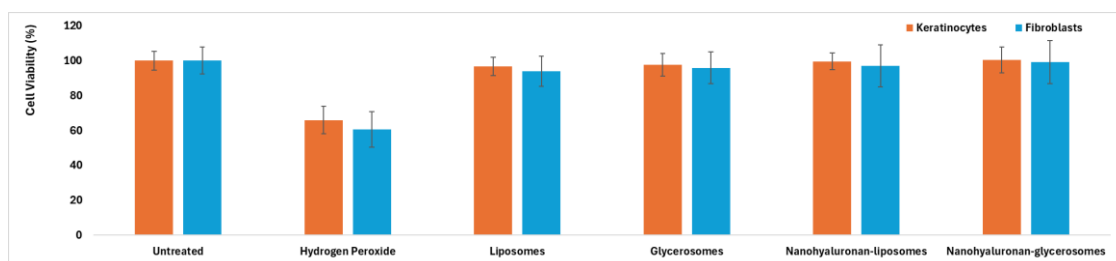


Figure 4. Viability of keratinocytes and fibroblasts stressed with hydrogen peroxide and treated for 4 h with curcumin (0.1 $\mu\text{g}/\text{ml}$) loaded in liposomes, glycerosomes, nanohyaluronan-liposomes and nanohyaluronan-glycerosomes. Each value represents the average \pm standard deviation of at least six determinations (n=9).

The viability of both cells treated with hydrogen peroxide decreased up to around 62% and the treatment with curcumin samples increased the value up to around 100% ($p < 0.05$ versus viability of untreated cells), thus restoring the healthy condition, irrespective of cells and formulation used (Figure 4).

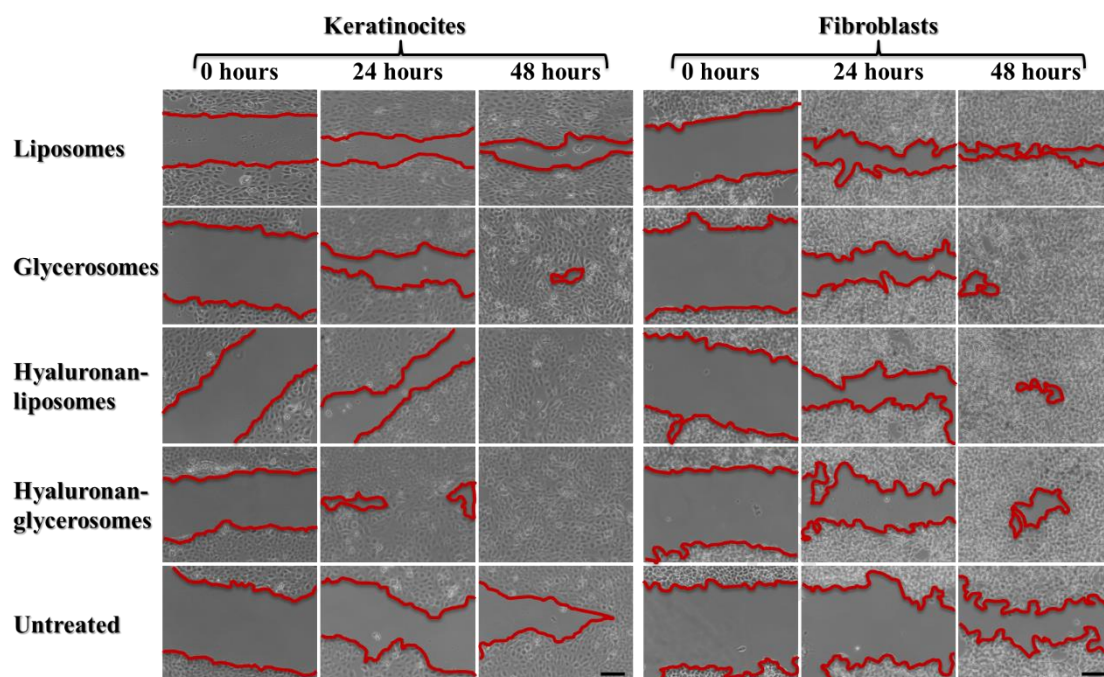


Figure 5. Representative microscopy images of scratch performed in monolayers of keratinocytes and fibroblasts untreated or treated for 48 h with curcumin loaded liposomes, glycerosomes, nanohyaluronan-liposomes and nanohyaluronan-glycerosomes. Scale bars: 100 μm .

The scratch assay confirmed a better closure of performed lesions, especially when curcumin was loaded in nanohyaluronan-liposomes and nanohyaluronan-glycerosomes (Figure 5), probably due to a better stimulation of the migration of these cells, speeding up the closure of the damaged areas.

In vivo studies

Macroscopic (gross) study

When the study was performed in healthy rats, on day 3, the measured areas of lesions were around 22000 μm^2 ($p > 0.05$ among the different areas), any statistically significant difference was found among the lesion areas untreated or treated with curcumin samples (Figure 6, left panel). On day 7, the lesion areas were reduced, around 12000 μm^2 ($p > 0.05$ among the different areas) but those treated with curcumin samples were not statistically different in comparison with the untreated ones. Differently, on day 14, the lesion areas treated with curcumin loaded in nanohyaluronan-glycerosomes were statistically different than that untreated or treated with the other curcumin samples, denoting a better and faster wound closure provided by this formulation.

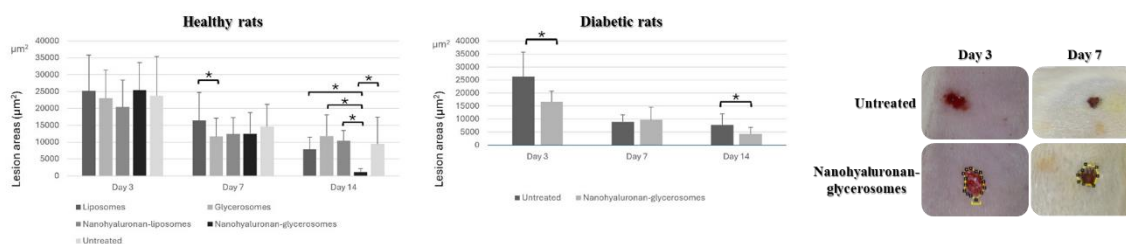


Figure 6. Representative images of lesion areas (right panel) and size (μm^2) of healthy (left panel) and diabetic rats (middle panel) untreated (controls) or topically treated with curcumin loaded in liposomes, glycosomes, nano-hyaluronan-liposomes and nano-hyaluronan-glycosomes. Mean values \pm standard deviations (error bars) are reported ($n=9$). Symbol * indicates values statistically different ($p<0.05$).

When the study was performed in diabetic rats, only curcumin loaded in nano-hyaluronan-glycosomes was used as this formulation provided the best results in healthy animals. Its values were compared with that of untreated animals (Figure 6, middle panel). On days 3 and 14, a significantly greater wound closure was found in animals treated with curcumin loaded in nano-hyaluronan-glycosomes (around $15000 \mu\text{m}^2$, at day 3, $p<0.05$ versus the value of untreated; around $4500 \mu\text{m}^2$, at day 14, $p<0.05$ versus the value of untreated) in comparison with untreated controls. Results were macroscopically confirmed by the images of skin lesions (Figure 6, right panel).

Microscopic study

In healthy rats, on day 3, the wounds of untreated control (14 mm, $p<0.05$ versus others) were significantly but only slightly larger than that of the groups that received curcumin loaded in liposomes (13 mm, $p<0.05$ versus others) and hyalurosomes (11 mm, $p<0.05$ versus others) (Figure 7). Differently the wounds of the animals treated with nano-hyaluronan-liposomes (9.3 mm, $p<0.05$ versus others) and nano-hyaluronan-glycosomes (8.5 mm, $p<0.05$ versus others) were clearly smaller than that of untreated animals ($p<0.05$). Likewise, on day 7 the wounds of each group were statistically different versus the other groups ($p<0.05$), and healing was seen to be most advanced in the rats treated with curcumin in liposomes (2 mm, $p<0.05$ versus others) and nano-hyaluronan-glycosomes (2.2 mm, $p<0.05$ versus others), confirming the ability of formulations to speed up the wound closure in comparison with the control. No difference between treated and untreated rats were detected at day 14.

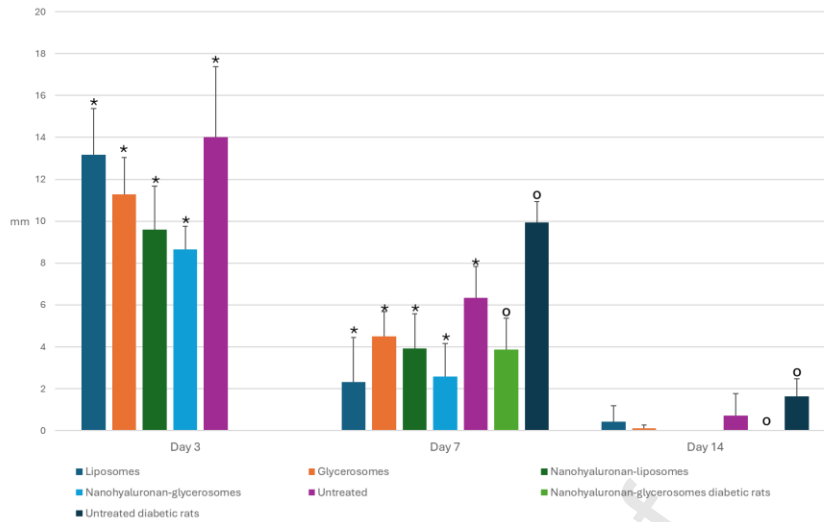


Figure 7. Re-epithelization quantified recording the distance (μm) between margins of the wounds by the ImageJ program in $3 \mu\text{m}$ sections of skin wounds stained with hematoxylin-eosin and previous untreated (control) or treated with curcumin loaded in liposomes, glycosomes, nano-hyaluronan-liposomes and nano-hyaluronan-glycosomes. Mean values \pm standard deviations (error bars) are reported ($n=9$). Symbol * indicates values statistically different ($p<0.05$).

In the diabetic rat model, treatment with curcumin loaded nano-hyaluronan-glycosomes clearly and significantly improved the re-epithelization area, at days 7 and 14, in comparison with the controls, Figure 7.

Immunohistochemical study

The wound tissues were cut, fixed, coloured with hematoxylin and eosin or Masson Trichrome staining and observed with an optical microscope (Figure 8). At all the timepoints of the study there were greater numbers of cell nuclei undergoing division at the epidermal margins of the wounds in the treated diabetic rats versus the diabetic controls, with statistically significant differences being observed on days 3 and 14.

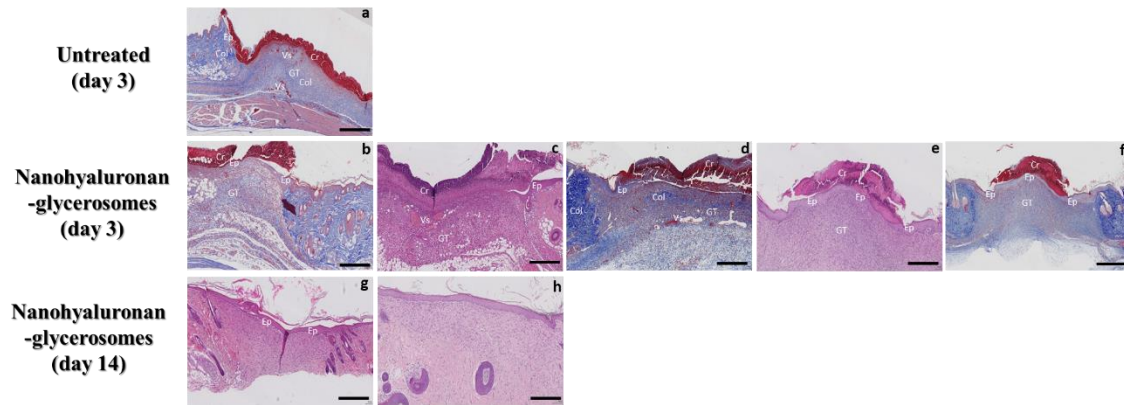


Figure 8. Representative images of 3 μm sections of skin wounds of heathy rats (a), and rats treated with nanohyaluronan-glycosomes (b, c, d, e, f) at day 3, and treated with nanohyaluronan-glycosomes (g and h) at day 14. Skin specimens were stained with hematoxylin and eosin (c, e, g, h) or Masson Trichrome staining (a, b, d, f). The main histopathological characteristics were underlined as granulation tissue (GT), serohematic crust (Cr), healthy epidermis (Ep), collagen (Col) and vascularization (Vs). Scale bars: 500 μm .

On day 3, the skin of untreated animals appeared ulcerated (everted edges) with immature granulation tissue (GT) (Figure 8 a, T.M. 4x). In the skin of rats treated with nanohyaluronan-glycosomes (Figure 8 c) the formation of a granulation tissue (GT) highly vascularized under a sero-hematic crust (Cr) was observed. The healthy epidermis (Ep) on the right border begin to proliferate under the scab (H.E. 10x). Normal collagenization (Masson Trichrome staining) of the dermis and the presence of skin appendages were observed (Figure 8 b, right side, T.M. 20x). Granulation tissue in the process of maturation (Figure 8 d, T.M. 10x) and re-epithelialization with presence of crust (Cr) were observed as well (Figure 8 e, H.E. 4x and f, T.M. 10x). On day 14, the skin of animals treated with nanohyaluronan-glycosomes appeared completely repaired without scab and surface keratin production (Figure 8 g, H.E. 4x and h, H.E. 10x).

Regarding the rest of the histopathological parameters, i.e., angiogenesis, granulation, collagen formation and inflammation, the results were more heterogeneous. A lesser presence of granulation tissue was observed on day 7 in skin treated with curcumin loaded nanohyaluronan-glycosomes, indicating faster wound maturation. Of note was the tendency towards increased angiogenesis in the early phases (day 3) in the animals

that received curcumin loaded nanohyaluronan-glycosomes, even if in no case statistical significance was reached (Figure 9). Any statistically significant differences were observed as well in TIMP-1, MMP-9 and CD-34 measured in the skin of animals untreated or treated with curcumin loaded nanohyaluronan-glycosomes (data not shown).

Diabetes had a clear negative impact upon neovascularization, with a greater area occupied by blood vessels being observed in the healthy rats than in the diabetic ones (untreated or treated) on days 7 and 14. However, in the animals treated with curcumin loaded nanohyaluronan-glycosomes the vascularization was slightly improved in treated diabetic rats in comparison with the control, while no difference between treated and untreated rats were detected at day 14 (Figure 9).

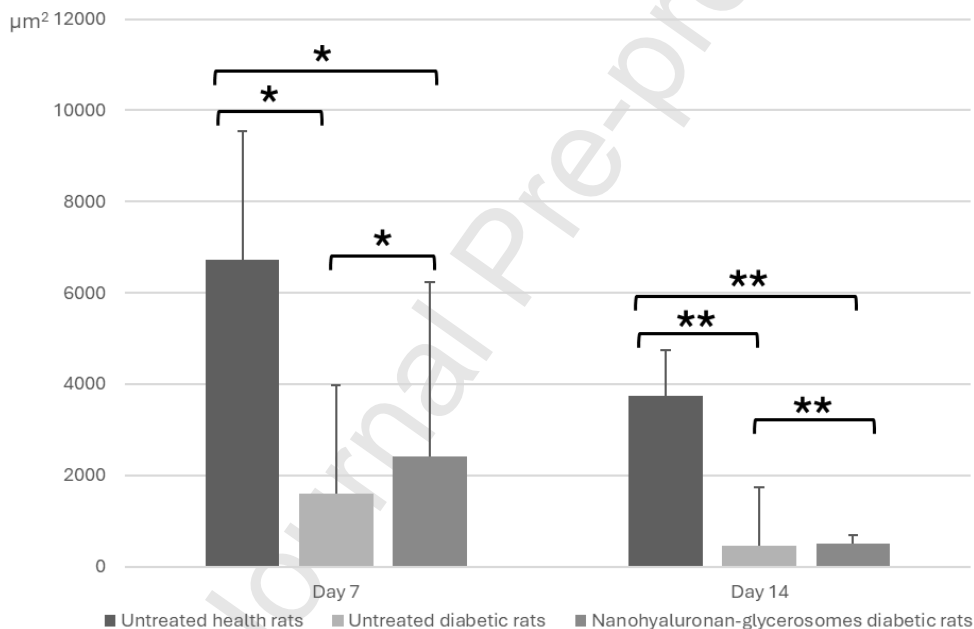


Figure 9. Vascularization area obtained quantifying the zone (μm^2) occupied by blood vessels randomly selected in three wound areas ($100 \mu\text{m}^2$ stained with hematoxylin-eosin) and untreated (control) or treated with curcumin loaded nanohyaluronan-glycosomes. Mean values \pm standard deviations (error bars) are reported (n=9). Symbols indicate values statistically different (*p<0.05; **p<0.001).

Discussion

Diabetes mellitus is a highly prevalent disease known for causing complications and impairing the healing process of wounds and ulcers. In 2015, the number of cases of this

pathology worldwide was approximately 415 million and is expected to reach 642 million by the year 2040 [26]. In diabetic patients it has been demonstrated that activity and migration of neutrophils, fibroblasts and leukocytes are altered at the ulcer site. Elderly adults with diabetes mellitus have a decrease in subcutaneous adipose tissue, the elastin fibres undergo fragmentation, and epidermal turnover and collagen production are less effective than in healthy individuals [27]. Thus, the early and effective treatment of these wounds is a therapeutic and economic challenge of the present century. Only in the United Kingdom, during the period 2014-2015, the cost of treating diabetic foot ulcers (including amputation surgery) ranged between 973 and 1120 million euros, representing 0.8-0.9% of the total National Health Service budget of this country [28].

Considering this important challenge, in the present study a new ad hoc formulated therapeutic formulation was developed loading curcumin in the self-assembled hyaluronan-cholesterol nanogel that was further combined with phospholipids with and without glycerol to obtain curcumin loaded nanohyaluronan-liposomes or nanohyaluronan-glycerolesomes. Their efficacy was assayed using a tissue repair model in healthy and diabetic rats, that is highly predictive as in these animals the repair is compromised like in humans (Figure 10).

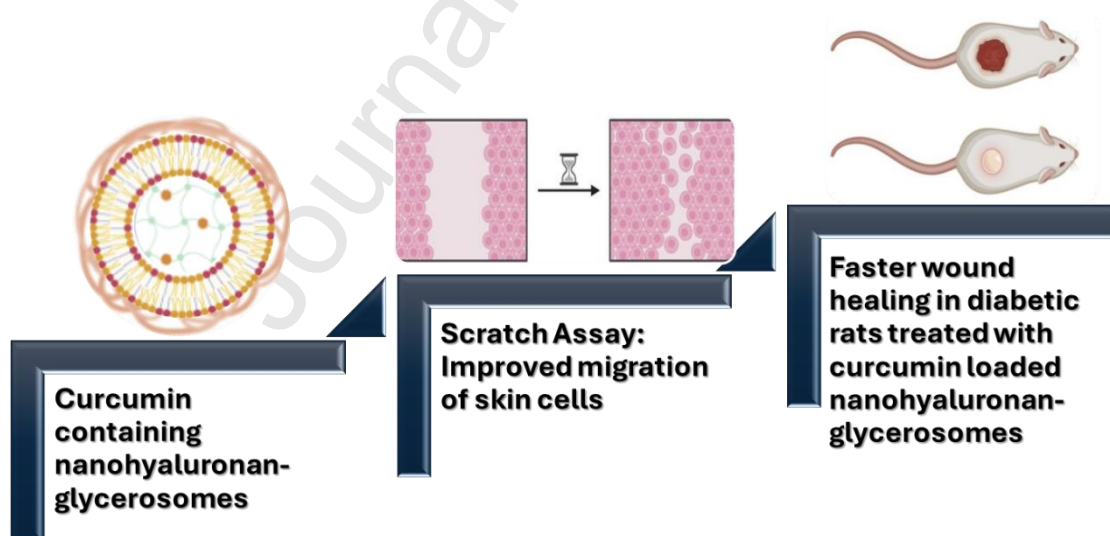


Figure 10. Schematic diagram of the system design and effectiveness

Taking into account the optimal results obtained in previous studies using hyalurosomes [16], phospholipid vesicles immobilized with hyaluronan, curcumin was selected as ideal bioactive molecule. Indeed, this magical phenol has multiple biological properties,

including antioxidant, anti-inflammatory, anti-bacterial, anti-diabetic, anti-fibrotic and anti-amyloid activities [10,29]. Specifically, on skin wounds, curcumin has also been associated with early apoptosis, reflecting rapid transition between the inflammatory phase and the proliferative phase of the wound healing process. It was loaded in nanohyaluronan-liposomes or nanohyaluronan-glycosomes as each of the components of these formulations can improve the skin penetration of payloads. Hyaluronan-cholesterol nanogels previously demonstrated their ability to cross the barrier-disrupted human skin (with partial removal and loosening of stratum corneum), up to the viable epidermis where are taken up by keratinocytes [30]. In mechanically produced wounds, nanohydrogels accumulated in tissue and are taken up by dermis cells, e.g. fibroblasts and phagocytic cells. Their cellular uptake is CD44-mediated, and it is more effective using hyaluronan in form of nanohydrogels, as reported in previous studies [31–33]. Phospholipids are the main components of cellular membrane and are present in the intracellular matrix of the first strata of viable epidermis. Thus, they can interact with this matrix, increasing its fluidity and permeability [34]. Glycerol is a humectant, naturally occurring in the skin and capable of improving the hydration of stratum corneum and enhancing desmosomal degradation, thus facilitating the removal of dead cells [35]. The combination of these three components in a unique formulation allowed the formation of spherical and multicompartiment vesicles sized ~543 nm and negatively charged. These vesicles stably loaded 10 mg/mL of curcumin and, when applied on the skin surface, delivered it along with the hydrophilic probe up to the viable epidermis. Analysing the obtained merged images of the skin treated with curcumin and carboxyfluorescein loaded in nanohyaluronan-glycosomes, it is possible to hypothesize that a part of the vesicles fused within the stratum corneum, and their components acted as penetration enhancer that destabilized the intercellular matrix and facilitated the passage of other vesicles up to the viable epidermis.

The prepared and tested curcumin loaded nanohyaluronan-liposomes and -glycosomes were biocompatible with keratinocytes and fibroblasts, which are the main representative cells of the skin, when used at concentration $\leq 10 \mu\text{g/mL}$. The lowest concentration of curcumin (0.1 $\mu\text{g/ml}$) was selected to evaluate the *in vitro* effectiveness of formulations, as it was the most reliable in terms of amount of curcumin capable of reaching the viable epidermis and interacting with cells upon topical application. At this concentration all the tested curcumin samples inhibited the mortality of cells

(keratinocytes and fibroblasts) caused by hydrogen peroxide, restoring the healthy conditions and reaching the same viability of unstressed cells. In this study the behaviour of curcumin loaded nanohyaluronan-glycosomes was comparable with that of other vesicles. Differently, testing the formulation ability to promote *in vitro* migration of keratinocytes and fibroblasts at the lesion surface, nanohyaluronan-liposomes and -glycosomes were more effective than the corresponding liposomes and glycosomes used as reference, probably due to the presence of hyaluronan nanohydrogel that can be easier internalized by the cells giving rise to improved biosynthesis of the extracellular matrix and tissue granulation [9,10,30].

Considering the promising results obtained *in vitro*, curcumin loaded nanohyaluronan-liposomes and -glycosomes were applied *in vivo* on the skin wounds of healthy and diabetic rats. The re-epithelization in the healthy rats treated with nanohyaluronan-glycosomes was macroscopically evident. In the diabetic ones, it seemed to be faster as wound size was lower at days 3 and 7. Similar results were obtained by Manca et al. (2015) [16]. They found that the loading of curcumin (10 mg/mL) in hyalurosomes, accelerated the healing process in mice, but they only tested the formulations in healthy mice. Sharma et al. (2018) [36] used diabetic animals and reported similar results, with faster healing in a diabetic model in which the full-thickness wounds were treated with a formulation of curcumin in hyaluronic acid. Similarly, Lin et al. (2017) [37] found faster healing of the wounded area of rats treated with curcumin contained in chitosan nanoparticles. Zhang et al. (2016) [38] employed a new curcumin derivative that had a zinc binding site, similar to that found in the tetracyclines, which had an inhibitory action upon the metalloproteinases. Its application to the wounds of diabetic rats significantly accelerated the healing process that was macroscopically evident and supported by the histomorphometric findings. Differently, comparable results were not obtained by Hamam et al. (2020) [39] that treated the wounds of Wistar rats with curcumin loaded in mesoporous silica, probably because these samples were not suitable for topical application.

Other factor that can influence the effectiveness of curcumin loaded nanohyaluronan-glycosomes is their ability to control the inflammation process. It usually develops in the first 24 h, with the recruitment of monocytes, macrophages and polymorphonuclear cells at the site of the wound, along with the activation of mast cells and Langerhans cells. In our study, despite the ability of formulations to deliver curcumin in the viable

epidermis and dermis, where it would reduce the inflammatory components during the wound healing process, the histopathological images did not reveal a decreased inflammation process at any of the studied timepoints. Nevertheless, Kamar et al. (2019) found that the formulation of curcumin nanoparticles that they used, reduced inflammation in the histological analysis of wounds in albino rats [40].

In addition, the diabetic rats treated with curcumin loaded hyaluronan-cholesterol nanogel had fewer vessels than the healthy controls on days 7 and 14, but the area occupied by blood vessels was significantly greater than that found in the untreated diabetic rats. These findings support the pro-angiogenic effect of curcumin and are consistent with those of previous studies such as those published by Hamam et al. (2020) [39] and Krausz et al. (2015) [41], both evidencing increased vessel formation in the wounds treated with curcumin loaded in nanoparticles. The start of angiogenesis is regulated by a number of soluble factors, including particularly VEGF-A, in response to tissue hypoxia at the site of the wound. Following an “explosive” growth of neo vessels, a vascular “trimming” process takes place until the vessel density becomes similar to that of the normal skin. Apoptosis and capillary maturation at the expense of the pericytes is crucial in this process [42].

Fibroblast maturation and number, and in this regard, the granulation tissue, composed of fibroblasts within a network of neo vessels and extracellular matrix, was seen to be less abundant in the healthy (non-diabetic) and untreated controls on day 3. This result indicates a delay in the healing process with respect to the other animals. On days 7 and 14 the granulation tissue was more abundant in the rats treated with curcumin loaded nanohyaluronan-glycosomes than in the untreated controls, suggesting that the repair process was more advanced in the treated animals. On day 7 the granulation tissue in the diabetic rats was found to be more abundant and mature when treated with curcumin loaded nanohyaluronan-glycosomes, in concordance with that obtained in the non-diabetic rats. In turn, on day 14, the rats treated with this formulation had less granulation tissue, which should relate to a more evolved repair process. Despite these findings, no statistically significant differences were observed, in the same way as in the study carried out by Hamam et al. (2020) [39]. On applying curcumin nanoparticles embedded in a dressing of collagen and polyvinyl alcohol, Leng et al. (2020) [43] likewise observed no statistically significant differences in the granulation process.

Collagenization forms part of the proliferative phase in which the fibroblasts recruited from the dermis at the wound margins produce mainly type III collagen, which is subsequently replaced by type I collagen. This protein represents 70-80% of the skin and is the most abundant protein in the extracellular matrix, suggesting the importance of its production during skin wound repair. In the present study, on day 3, collagen accumulation in untreated rats was much lower than in most of the rats treated with curcumin samples, while in diabetic rats collagenization was seen to be greater on day 14 among the treated animals. This delay in collagen synthesis could be explained by the difficulty of tissue repair in the context of diabetes. These findings are consistent with those published by Leng et al. (2020) [43], since the application of curcumin nanoparticles did not result in increased wound collagenization in the rats compared with those treated with a dressing of collagen and polyvinyl alcohol, or with a dressing alone. In contrast to Hamam et al. (2005) [39], Krausz et al. (2015) [41] and Lin et al. (2017) [37], no statistically significant differences were found in relation to this parameter, though the data obtained suggest that collagenization may occur earlier in the treated groups than among the controls. Zhang et al. (2016) [38] evaluated the accumulation of collagen in the wounds of diabetic rats by quantifying hydroxyproline and found accumulation to be lower in the diabetic rats than in the healthy animals. However, in the treated diabetic rats the amount of collagen increased significantly during the study. On the other hand, Zahiri et al. (2020) [44] applied curcumin loaded in chitosan nanoparticles to the wounds of Wistar rats, and recorded significantly greater collagen production than in the untreated animals.

Despite the promising results, it is necessary to underline that the duration of the present study was limited to 14 days versus other studies involving periods of 30 days [45], which in turn may have limited the demonstration of statistically significant differences, especially in the diabetic animals. This is because of the well-known negative and delaying effects of hyperglycemia upon the healing process, including leukocyte dysfunction, altered fibroblast activity and collagen synthesis, keratinocyte differentiation and migration disorders, endothelial dysfunction, etc. On the other hand, despite its many advantages, the use of a rat model does not allow the direct extrapolation of findings to human skin under similar conditions. Indeed, there are some inter-species differences in the healing processes and phases, since the primary healing

mechanism in rodents is wound contraction, whereas in humans, up to 80% of the wound heals through re-epithelialization.

Conclusions

Considering the interesting findings obtained, it is possible to conclude that curcumin delivered in a new kind of vesicles, called nanohyaluronan-glycosomes and prepared combining hyaluronan-cholesterol nanohydrogel with phospholipid and glycerol, represent a suitable option to be taken into account for improving skin regeneration and repair, though further studies are needed, involving techniques capable of clarifying the underlying mechanisms of action and establishing the appropriate dosing specifications.

Journal Pre-proof

References

- [1] J.L. Bologna, J. V Schaffer, L. Cerroni, *Dermatology 2: Volume set, 4th Edition*, in: *Dermatology*, 2018.
- [2] F.A.K.D.H.S.L.D.J.J. Loscalzo J, Harrison. *Principios de Medicina Interna*, n.d.
- [3] N. Dasari, A. Jiang, A. Skochdopole, J. Chung, E.M. Reece, J. Vorstenbosch, S. Winocour, *Updates in Diabetic Wound Healing, Inflammation, and Scarring, Semin Plast Surg* 35 (2021) 153–158. <https://doi.org/10.1055/s-0041-1731460>.
- [4] J. Holl, C. Kowalewski, Z. Zimek, P. Fiedor, A. Kaminski, T. Oldak, M. Moniuszko, A. Eljaszewicz, *Chronic Diabetic Wounds and Their Treatment with Skin Substitutes, Cells* 10 (2021) 655. <https://doi.org/10.3390/cells10030655>.
- [5] M. Allaw, M. Pleguezuelos-Villa, M.L. Manca, C. Caddeo, M. Aroffu, A. Nacher, O. Diez-Sales, A.R. Saurí, E.E. Ferrer, A.M. Fadda, M. Manconi, *Innovative strategies to treat skin wounds with mangiferin: Fabrication of transfersomes modified with glycols and mucin, Nanomedicine* 15 (2020) 1671–1685. <https://doi.org/10.2217/NNM-2020-0116>.
- [6] J.B. Johnson, D.A. Broszczak, J.S. Mani, J. Anesi, M. Naiker, *A cut above the rest: oxidative stress in chronic wounds and the potential role of polyphenols as therapeutics, Journal of Pharmacy and Pharmacology* 74 (2022) 485–502. <https://doi.org/10.1093/jpp/rgab038>.
- [7] A. Martelli, L. Flori, E. Gorica, E. Piragine, A. Saviano, G. Annunziata, M.N.D. Di Minno, R. Ciampaglia, I. Calcaterra, F. Maione, G.C. Tenore, E. Novellino, V. Calderone, *Vascular Effects of the Polyphenolic Nutraceutical Supplement Taurisolo®: Focus on the Protection of the Endothelial Function, Nutrients* 13 (2021) 1540. <https://doi.org/10.3390/nu13051540>.
- [8] K.M. Nelson, J.L. Dahlin, J. Bisson, J. Graham, G.F. Pauli, M.A. Walters, *The Essential Medicinal Chemistry of Curcumin, J Med Chem* 60 (2017) 1620–1637. <https://doi.org/10.1021/acs.jmedchem.6b00975>.
- [9] C. Mohanty, S.K. Sahoo, *Curcumin and its topical formulations for wound healing applications, Drug Discov Today* 22 (2017) 1582–1592. <https://doi.org/10.1016/j.drudis.2017.07.001>.
- [10] D. Akbik, M. Ghadiri, W. Chrzanowski, R. Rohanizadeh, *Curcumin as a wound healing agent, Life Sci* 116 (2014) 1–7. <https://doi.org/10.1016/j.lfs.2014.08.016>.
- [11] R.L. Thangapazham, S. Sharad, R.K. Maheshwari, *Phytochemicals in Wound Healing, Adv Wound Care (New Rochelle)* 5 (2016) 230–241. <https://doi.org/10.1089/wound.2013.0505>.
- [12] Y. He, Y. Yue, X. Zheng, K. Zhang, S. Chen, Z. Du, *Curcumin, Inflammation, and Chronic Diseases: How Are They Linked?, Molecules* 20 (2015) 9183–9213. <https://doi.org/10.3390/molecules20059183>.
- [13] Q. Wei, Y. Zhao, Y. Wei, Y. Wang, Z. Jin, G. Ma, Y. Jiang, W. Zhang, Z. Hu, *Facile preparation of polyphenol-crosslinked chitosan-based hydrogels for cutaneous wound*

- repair, *Int J Biol Macromol* 228 (2023) 99–110.
<https://doi.org/10.1016/j.ijbiomac.2022.12.215>.
- [14] C. Quispe, N. Cruz-Martins, M.L. Manca, M. Manconi, O. Sytar, N. Hudz, M. Shanaida, M. Kumar, Y. Taheri, M. Martorell, J. Sharifi-Rad, G. Pintus, W.C. Cho, Nano-Derived Therapeutic Formulations with Curcumin in Inflammation-Related Diseases, *Oxid Med Cell Longev* 2021 (2021). <https://doi.org/10.1155/2021/3149223>.
- [15] X. Wang, R. Li, H. Zhao, Enhancing angiogenesis: Innovative drug delivery systems to facilitate diabetic wound healing, *Biomedicine & Pharmacotherapy* 170 (2024) 116035. <https://doi.org/10.1016/j.biopha.2023.116035>.
- [16] M.L. Manca, I. Castangia, M. Zaru, A. Nacher, D. Valenti, X. Fernandez-Busquets, A. m. Fadda, M. Manconi, Development of curcumin loaded sodium hyaluronate immobilized vesicles (hyalurosomes) and their potential on skin inflammation and wound restoring., *Biomaterials* 71 (2015) 100–109.
- [17] M.L. Manca, D. Lattuada, D. Valenti, O. Marelli, C. Corradini, X. Fernàndez-Busquets, M. Zaru, A.M. Maccioni, A.M. Fadda, M. Manconi, Potential therapeutic effect of curcumin loaded hyalurosomes against inflammatory and oxidative processes involved in the pathogenesis of rheumatoid arthritis: The use of fibroblast-like synovial cells cultured in synovial fluid, *European Journal of Pharmaceutics and Biopharmaceutics* 136 (2019). <https://doi.org/10.1016/j.ejpb.2019.01.012>.
- [18] E. Montanari, N. Zoratto, L. Mosca, L. Cervoni, E. Lallana, R. Angelini, R. Matassa, T. Coviello, C. Di Meo, P. Matricardi, Halting hyaluronidase activity with hyaluronan-based nanohydrogels: development of versatile injectable formulations, *Carbohydr Polym* 221 (2019) 209–220. <https://doi.org/10.1016/j.carbpol.2019.06.004>.
- [19] S. Mir-palomo, A. Nàcher, O. Díez-sales, M.A.O. Vila, C. Caddeo, M. Letizia, M. Manconi, A. Maria, Inhibition of skin inflammation by baicalin ultradeformable vesicles, *Int J Pharm* 511 (2016) 23–29. <https://doi.org/10.1016/j.ijpharm.2016.06.136>.
- [20] M.L. Manca, M. Manconi, A.M. Falchi, I. Castangia, D. Valenti, S. Lampis, A.M. Fadda, Close-packed vesicles for diclofenac skin delivery and fibroblast targeting, *Colloids Surf B Biointerfaces* 111 (2013) 609–617. <https://doi.org/http://dx.doi.org/10.1016/j.colsurfb.2013.07.014>.
- [21] Y. Abramov, B. Golden, M. Sullivan, S.M. Botros, J.R. Miller, A. Alshahrour, R.P. Goldberg, P.K. Sand, Histologic characterization of vaginal vs. abdominal surgical wound healing in a rabbit model, *Wound Repair and Regeneration* 15 (2007) 80–86. <https://doi.org/10.1111/j.1524-475X.2006.00188.x>.
- [22] C.J. Newcomb, T.J. Moyer, S.S. Lee, S.I. Stupp, Advances in cryogenic transmission electron microscopy for the characterization of dynamic self-assembling nanostructures, *Curr Opin Colloid Interface Sci* 17 (2012) 350–359. <https://doi.org/10.1016/j.cocis.2012.09.004>.
- [23] A. Catalan-Latorre, M. Ravaghi, M.L. Manca, C. Caddeo, F. Marongiu, G. Ennas, E. Escribano-Ferrer, J.E. Peris, O. Díez-Sales, A.M. Fadda, M. Manconi, Freeze-dried eudragit-hyaluronan multicompartiment liposomes to improve the intestinal

- bioavailability of curcumin, *European Journal of Pharmaceutics and Biopharmaceutics* 107 (2016) 49–55. <https://doi.org/10.1016/j.ejpb.2016.06.016>.
- [24] M. Manconi, M.L. Manca, C. Caddeo, D. Valenti, C. Cencetti, O. Diez-Sales, A. Nacher, S. Mir-Palomo, M.C. Terencio, D. Demurtas, J.C. Gomez-Fernandez, F.J. Aranda, A.M. Fadda, P. Matricardi, Nanodesign of new self-assembling core-shell gellan-transfersomes loading baicalin and in vivo evaluation of repair response in skin, *Nanomedicine* 14 (2018) 569–579. <https://doi.org/10.1016/j.nano.2017.12.001>.
- [25] J. López-García, M. Lehocký, P. Humpolíček, P. Sáha, HaCaT Keratinocytes Response on Antimicrobial Atelocollagen Substrates: Extent of Cytotoxicity, Cell Viability and Proliferation, *J Funct Biomater* 5 (2014) 43–57. <https://doi.org/10.3390/jfb5020043>.
- [26] P. Zimmet, K.G. Alberti, D.J. Magliano, P.H. Bennett, Diabetes mellitus statistics on prevalence and mortality: facts and fallacies, *Nat Rev Endocrinol* 12 (2016) 616–622. <https://doi.org/10.1038/nrendo.2016.105>.
- [27] T. Sheleme, G. Mamo, T. Melaku, T. Sahilu, <p>Prevalence, Patterns and Predictors of Chronic Complications of Diabetes Mellitus at a Large Referral Hospital in Ethiopia: A Prospective Observational Study</p>, *Diabetes Metab Syndr Obes* Volume 13 (2020) 4909–4918. <https://doi.org/10.2147/DMSO.S281992>.
- [28] L. Barnsbee, Q. Cheng, R. Tulleners, X. Lee, D. Brain, R. Pacella, Measuring costs and quality of life for venous leg ulcers, *Int Wound J* 16 (2019) 112–121. <https://doi.org/10.1111/iwj.13000>.
- [29] M. Barchitta, A. Maugeri, G. Favara, R. Magnano San Lio, G. Evola, A. Agodi, G. Basile, Nutrition and Wound Healing: An Overview Focusing on the Beneficial Effects of Curcumin, *Int J Mol Sci* 20 (2019) 1119. <https://doi.org/10.3390/ijms20051119>.
- [30] E. Montanari, P. Mancini, F. Galli, M. Varani, I. Santino, T. Coviello, L. Mosca, P. Matricardi, F. Rancan, C. Di Meo, Biodistribution and intracellular localization of hyaluronan and its nanogels. A strategy to target intracellular *S. aureus* in persistent skin infections, *Journal of Controlled Release* 326 (2020) 1–12. <https://doi.org/10.1016/j.jconrel.2020.06.007>.
- [31] R. Racine, M. E., Hyaluronan Endocytosis: Mechanisms of Uptake and Biological Functions, in: *Molecular Regulation of Endocytosis*, InTech, 2012. <https://doi.org/10.5772/45976>.
- [32] H. Ponta, L. Sherman, P.A. Herrlich, CD44: From adhesion molecules to signalling regulators, *Nat Rev Mol Cell Biol* 4 (2003) 33–45. <https://doi.org/10.1038/nrm1004>.
- [33] E. Montanari, P. Mancini, F. Galli, M. Varani, I. Santino, T. Coviello, L. Mosca, P. Matricardi, F. Rancan, C. Di Meo, Biodistribution and intracellular localization of hyaluronan and its nanogels. A strategy to target intracellular *S. aureus* in persistent skin infections, *Journal of Controlled Release* 326 (2020) 1–12. <https://doi.org/10.1016/j.jconrel.2020.06.007>.
- [34] Y. Yokomizo, Effects of phospholipids on the percutaneous penetration of drugs through the dorsal skin of the guinea pig, in vitro. 3. The effects of phospholipids on

- several drugs having different polarities, *Journal of Controlled Release* 42 (1996) 217–228. [https://doi.org/10.1016/0168-3659\(96\)01347-8](https://doi.org/10.1016/0168-3659(96)01347-8).
- [35] J.W. Fluhr, R. Darlenski, C. Surber, Glycerol and the skin: holistic approach to its origin and functions, *British Journal of Dermatology* 159 (2008) 23–34. <https://doi.org/10.1111/j.1365-2133.2008.08643.x>.
- [36] M. Sharma, K. Sahu, S.P. Singh, B. Jain, Wound healing activity of curcumin conjugated to hyaluronic acid: *in vitro* and *in vivo* evaluation, *Artif Cells Nanomed Biotechnol* 46 (2018) 1009–1017. <https://doi.org/10.1080/21691401.2017.1358731>.
- [37] Y. Lin, J. Lin, Y. Hong, Development of chitosan/poly- γ -glutamic acid/pluronic/curcumin nanoparticles in chitosan dressings for wound regeneration, *J Biomed Mater Res B Appl Biomater* 105 (2017) 81–90. <https://doi.org/10.1002/jbm.b.33394>.
- [38] Y. Zhang, S.A. McClain, H.-M. Lee, M.S. Elburki, H. Yu, Y. Gu, Y. Zhang, M. Wolff, F. Johnson, L.M. Golub, A Novel Chemically Modified Curcumin “Normalizes” Wound-Healing in Rats with Experimentally Induced Type I Diabetes: Initial Studies, *J Diabetes Res* 2016 (2016) 1–11. <https://doi.org/10.1155/2016/5782904>.
- [39] F. Hamam, A. Nasr, Curcumin-loaded mesoporous silica particles as wound-healing agent: An *In vivo* study, *Saudi J Med Med Sci* 8 (2020) 17. https://doi.org/10.4103/sjmms.sjmms_2_19.
- [40] S.S. Kamar, D.H. Abdel-Kader, L.A. Rashed, Beneficial effect of Curcumin Nanoparticles-Hydrogel on excisional skin wound healing in type-I diabetic rat: Histological and immunohistochemical studies, *Annals of Anatomy - Anatomischer Anzeiger* 222 (2019) 94–102. <https://doi.org/10.1016/j.aanat.2018.11.005>.
- [41] A.E. Krausz, B.L. Adler, V. Cabral, M. Navati, J. Doerner, R.A. Charafeddine, D. Chandra, H. Liang, L. Gunther, A. Clendaniel, S. Harper, J.M. Friedman, J.D. Nosanchuk, A.J. Friedman, Curcumin-encapsulated nanoparticles as innovative antimicrobial and wound healing agent, *Nanomedicine* 11 (2015) 195–206. <https://doi.org/10.1016/j.nano.2014.09.004>.
- [42] L.A. DiPietro, Angiogenesis and wound repair: when enough is enough, *J Leukoc Biol* 100 (2016) 979–984. <https://doi.org/10.1189/jlb.4MR0316-102R>.
- [43] Q. Leng, Y. Li, X. Pang, B. Wang, Z. Wu, Y. Lu, K. Xiong, L. Zhao, P. Zhou, S. Fu, Curcumin nanoparticles incorporated in PVA/collagen composite films promote wound healing, *Drug Deliv* 27 (2020) 1676–1685. <https://doi.org/10.1080/10717544.2020.1853280>.
- [44] M. Zahiri, M. Khanmohammadi, A. Goodarzi, S. Ababzadeh, M. Sagharjoghi Farahani, S. Mohandesnezhad, N. Bahrami, I. Nabipour, J. Ai, Encapsulation of curcumin loaded chitosan nanoparticle within poly (ϵ -caprolactone) and gelatin fiber mat for wound healing and layered dermal reconstitution, *Int J Biol Macromol* 153 (2020) 1241–1250. <https://doi.org/10.1016/j.ijbiomac.2019.10.255>.
- [45] K. Zhang, Y. Zhang, Z. Li, N. Li, N. Feng, Essential oil-mediated glycosomes increase transdermal paeoniflorin delivery: optimization, characterization, and evaluation *in vitro* and *in vivo*, *Int J Nanomedicine* Volume 12 (2017) 3521–3532. <https://doi.org/10.2147/IJN.S135749>.

- [46] V. Kant, A. Gopal, N.N. Pathak, P. Kumar, S.K. Tandan, D. Kumar, Antioxidant and anti-inflammatory potential of curcumin accelerated the cutaneous wound healing in streptozotocin-induced diabetic rats, *Int Immunopharmacol* 20 (2014) 322–330. <https://doi.org/10.1016/j.intimp.2014.03.009>.
- [47] Z. Mohammadi, M. Sharif Zak, H. Majdi, E. Mostafavi, M. Barati, H. Lotfimehr, K. Ghaseminasab, H. Pazoki-Toroudi, T.J. Webster, A. Akbarzadeh, The effect of chrysin–curcumin-loaded nanofibres on the wound-healing process in male rats, *Artif Cells Nanomed Biotechnol* 47 (2019) 1642–1652. <https://doi.org/10.1080/21691401.2019.1594855>.

Journal Pre-proof

Declaration of interests

The authors declare that they have no known competing financial interests or personal relationships that could have appeared to influence the work reported in this paper.

The authors declare the following financial interests/personal relationships which may be considered as potential competing interests:

Journal Pre-proof